Clinical Biomechanics 33 (2016) 34–41

Contents lists available at ScienceDirect

Clinical Biomechanics

journal homepage: www.elsevier.com/locate/clinbiomech

Research paper

Compensatory strategies during manual wheelchair propulsion in response to weakness in individual muscle groups: A simulation study

Jonathan S. Slowik [a], Jill L. McNitt-Gray [b,c], Philip S. Requejo [d,e], Sara J. Mulroy [d], Richard R. Neptune [a,*]

[a] Department of Mechanical Engineering, The University of Texas at Austin, Austin, TX, USA
[b] Department of Biomedical Engineering, The University of Southern California, Los Angeles, CA, USA
[c] Department of Biological Sciences, The University of Southern California, Los Angeles, CA, USA
[d] Pathokinesiology Laboratory, Rancho Los Amigos National Rehabilitation Center, Downey, CA, USA
[e] Rehabilitation Engineering, Rancho Los Amigos National Rehabilitation Center, Downey, CA, USA

ARTICLE INFO

Article history:
Received 11 August 2015
Accepted 11 February 2016

Keywords:
Wheelchair propulsion
Forward dynamics simulation
Musculoskeletal model
Muscle weakness
Muscle fatigue
Biomechanics

ABSTRACT

Background: The considerable physical demand placed on the upper extremity during manual wheelchair propulsion is distributed among individual muscles. The strategy used to distribute the workload is likely influenced by the relative force-generating capacities of individual muscles, and some strategies may be associated with a higher injury risk than others. The objective of this study was to use forward dynamics simulations of manual wheelchair propulsion to identify compensatory strategies that can be used to overcome weakness in individual muscle groups and identify specific strategies that may increase injury risk. Identifying these strategies can provide rationale for the design of targeted rehabilitation programs aimed at preventing the development of pain and injury in manual wheelchair users.
Methods: Muscle-actuated forward dynamics simulations of manual wheelchair propulsion were analyzed to identify compensatory strategies in response to individual muscle group weakness using individual muscle mechanical power and stress as measures of upper extremity demand.
Findings: The simulation analyses found the upper extremity to be robust to weakness in any single muscle group as the remaining groups were able to compensate and restore normal propulsion mechanics. The rotator cuff muscles experienced relatively high muscle stress levels and exhibited compensatory relationships with the deltoid muscles.
Interpretation: These results underline the importance of strengthening the rotator cuff muscles and supporting muscles whose contributions do not increase the potential for impingement (i.e., the thoracohumeral depressors) and minimize the risk of upper extremity injury in manual wheelchair users.

1. Introduction

Over half of all manual wheelchair users will develop upper extremity pain and injury at some point in their lifetime (e.g., Finley and Rodgers 2004), which can be highly debilitating and lead to a decrease in independence and quality of life (e.g., Gutierrez et al. 2007). This high incidence of pain and injury is correlated with the considerable physical demand placed on the upper extremity during wheelchair propulsion (e.g., Curtis et al. 1999), as significant intermuscular coordination is needed to generate the mechanical power necessary to propel the wheelchair while maintaining joint stability (e.g., Rankin et al. 2010, 2011, 2012; van der Helm and Veeger 1996).

Many different combinations of muscle forces can produce the same net joint moments and generate the required mechanical power (e.g., Pandy and Andriacchi 2010). Although there is some uncertainty in how the neuromuscular system selects a particular combination of muscle forces to perform a given movement task, most theories suggest that the relative levels of force-generating capacity in individual muscles influence the selection (Erdemir et al. 2007). Muscle weakness (or decrease in the capacity to generate force) can be influenced by a number of factors including fatigue and neurological deficits (Requejo et al. 2008).

Muscle fatigue can result from a number of mechanisms, but it is generally quantified as a transient reduction in the force capacity of a muscle due to sustained physical activity (Enoka and Duchateau 2008). In order to fulfill specific task requirements, fatigue may occur at different rates in individual muscles and resulting fatigue-related changes in musculoskeletal loading may lead to injury (e.g., Kumar 2001). However, the overall effect of fatigue on wheelchair propulsion biomechanics is not well understood, as one study concluded that fatigue may lead to potentially harmful changes in propulsion mechanics (Rodgers et al. 1994), while others have suggested that during an

* Corresponding author at: Department of Mechanical Engineering, The University of Texas at Austin, 204 E. Dean Keeton Street, Stop C2200, Austin, TX 78712, USA.
E-mail address: rneptune@mail.utexas.edu (R.R. Neptune).

http://dx.doi.org/10.1016/j.clinbiomech.2016.02.003
0268-0033/

extended period of propulsion, individuals may actually make beneficial adjustments to their propulsion mechanics to mitigate the increased risk of injury (Rice et al. 2009). A number of inverse dynamics-based analyses have found that during manual wheelchair propulsion, the highest net joint moments and powers are generated at the shoulder, suggesting that the glenohumeral joint may be the most at risk for overuse injury (e.g., Rodgers et al. 1994; Veeger et al. 1991). These analyses also identified small fatigue-related shifts in joint power from the glenohumeral joint to more distal joints (Rodgers et al. 2003). Recently, Qi et al. (2012) found that electromyography intensity increases with fatigue and suggested that fatigue may contribute to imbalances between the contact and recovery phase muscles. However, the effect of fatigue in individual muscles on propulsion mechanics has remained relatively unexplored.

Muscle weakness can also result from neurological deficiencies due to injury or disease and ensuing neuromuscular changes, such as denervation and atrophy (e.g., Thomas and Zijdewind 2006). Furthermore, the breadth and magnitude of these reductions can vary based on the specific impairment or injury level. For example, a person with paraplegia will likely be able to produce larger forces with their triceps and pectoralis major muscles than a person with tetraplegia (e.g., van Drongelen et al. 2006). However, despite these differences, glenohumeral joint kinematic patterns and net joint moments during wheelchair propulsion have been shown to be remarkably similar across different spinal cord injury levels (Kulig et al. 2001; Newsam et al. 1999).

Although different combinations of muscle forces can produce the same net joint moments and minimize the effect of individual muscle weakness on propulsion mechanics, it is important to understand the potential compensatory strategies used by the neuromuscular system, as the resulting combinations of muscle forces may put the upper extremity at a higher risk for the development of pain and injury. The potential for injury has been highlighted in previous studies showing that joint instability due to larger forces from the deltoid relative to the humeral head depressors (i.e., rotators and adductors) may lead to subacromial impingement (e.g., Burnham et al. 1993; Sharkey and Marder 1995) and that other unbalanced combinations of forces can lead to dislocation (Labriola et al. 2005). These conditions are also related to the high prevalence of rotator cuff tears among manual wheelchair users (Morrow et al. 2014).

Forward dynamics simulations have been shown to be an effective tool to advance our understanding of intermuscular coordination during wheelchair propulsion (e.g., Rankin et al. 2011; Zajac et al. 2002). Potential compensatory strategies in response to individual muscle weakness can be revealed through analyzing the resulting shifts in individual muscle activation or power generation. A similar approach has previously been used to determine the effect of muscle weakness during steady-state walking (Goldberg and Neptune 2007; Jonkers et al. 2003; van der Krogt et al. 2012). Forward dynamics simulations can also be used to examine specific measures of upper extremity demand, such as muscle stress, to help identify muscles that may be placed at risk for overuse injuries (Rankin et al. 2012).

The purpose of this study was to use musculoskeletal modeling and forward dynamics simulations of wheelchair propulsion to identify potential compensatory strategies necessary to overcome weakness in individual muscle groups and highlight those strategies that could lead to the development of upper extremity pain and injury. The results of this study can provide rationale for the design of targeted rehabilitation programs aimed at minimizing the development of pain and injury in manual wheelchair users.

2. Methods

2.1. Musculoskeletal model

The upper extremity musculoskeletal model and dynamic optimization framework used in this study to generate the simulations of manual wheelchair propulsion have been previously described in detail (Rankin et al. 2010, 2011). The musculoskeletal model was developed using SIMM (Musculographics, Inc., Santa Rosa, CA, USA) based on the work of Holzbaur et al. (2005) and consisted of segments representing the trunk and right upper arm, forearm and hand. There were six rotational degrees-of-freedom representing trunk lean, shoulder plane of elevation, shoulder elevation angle, shoulder internal–external rotation, elbow flexion–extension, and forearm pronation–supination. The shoulder angles were the thoracohumeral angles, while the scapulohumeral rhythm was defined using regression equations based on cadaver data (de Groot and Brand 2001). Full-cycle trunk lean and contact-phase hand translations were prescribed based on experimentally measured kinematic data. The dynamic equations of motion were generated using SD/FAST (Parametric Technology Corp., Needham, MA, USA). Twenty-six Hill-type musculotendon actuators, governed by intrinsic muscle force-length-velocity and tendon force-strain relationships, represented the major upper extremity muscles crossing the shoulder and elbow joints (e.g., Slowik and Neptune 2013). Each actuator received a distinct excitation signal except the two sternocostal pectoralis major actuators, the three latissimus dorsi actuators, and the two actuators representing the lateral triceps and anconeus. Within each of these groups, the actuators received the same excitation signal, resulting in a total of 22 excitation groups. Muscle excitation–activation dynamics were modeled using a first order differential equation (Raasch et al. 1997) with muscle-specific activation and deactivation time constants (Happee and van der Helm 1995; Winters and Stark 1988). The musculotendon lengths and moment arms were determined using polynomial regression equations (Rankin and Neptune 2012) and the product of the appropriate muscle moment arm and force determined the muscle moment that was applied to each joint. In addition, passive torques were applied at the joints to represent ligaments and other passive joint structures that limit extreme joint positions (Davy and Audu 1987).

2.2. Simulation and optimization framework

Each muscle excitation pattern was generated using a bimodal pattern defined by six parameters (Hall et al. 2011), resulting in a total of 132 optimization parameters. A simulated annealing optimization algorithm (Goffe et al. 1994) was used to identify the excitation parameters that produced a simulation that best emulated the group-averaged experimental propulsion data (i.e., joint angle and 3D handrim force profiles; see Section 2.3 below) using an optimal tracking cost function (Neptune et al. 2001). An additional term was included in the cost function that minimized the square of muscle stress to prevent unnecessary co-contraction.

Based on a combination of anatomical location and muscle function, the musculotendon actuators were assigned to 12 muscle groups for analysis (Table 1). An initial simulation was generated using a set of baseline isometric muscle force values in the musculoskeletal model based on anatomical studies (Holzbaur et al. 2005; Table 1). These values were then systematically reduced by 50% one group at a time with the remaining groups left unaltered. The 50% reduction was deemed large enough to provide a meaningful difference and realistic in that it falls within the range of values reported in the literature due to fatigue from similar submaximal tasks (e.g., Enoka and Duchateau 2008). The excitation pattern of the weakened group was constrained to remain at the baseline values so that it could not compensate for itself, and the muscle excitation patterns of the remaining groups were re-optimized in order to restore the propulsion mechanics that emulated the experimental propulsion data, resulting in an additional 12 simulations.

2.3. Experimental data

To provide tracking data for the dynamic optimization, experimental data from twelve experienced male manual wheelchair users with

Table 1
Upper extremity muscle and group definitions.

Muscle group	Muscle	Compartment	Abbreviation	Origin	Insertion	Maximum isometric force (N)
ADelt	Deltoid	Anterior	DELT1	Clavicle	Humerus	1142.6
MDelt	Deltoid	Middle	DELT2	Scapula	Humerus	1142.6
		Posterior	DELT3	Scapula	Humerus	259.9
Subsc	Subscapularis	————————-	SUBSC	Scapula	Humerus	1377.8
Supra	Supraspinatus	————————-	SUPSP	Scapula	Humerus	487.8
Infra	Infraspinatus	————————-	INFSP	Scapula	Humerus	1210.8
	Teres Minor	————————-	TMIN	Scapula	Humerus	354.3
PecMaj	Pectoralis major	Clavicular head	PECM1	Clavicle	Humerus	364.4
		Sternocostal head - sternum	PECM2	Thorax	Humerus	515.4
		Sternocostal head - ribs	PECM3	Thorax	Humerus	390.6
	Coracobrachialis	————————-	CORB	Scapula	Humerus	242.5
Lat	Latissimus dorsi	Thoracic	LAT1	Thorax	Humerus	389.1
		Lumbar	LAT2	Thorax	Humerus	389.1
		Iliac	LAT3	Thorax	Humerus	281.7
	Teres Major	————————-	TMAJ	Scapula	Humerus	425.4
Tri	Triceps brachii	Long head	TRIlong	Scapula	Ulna	798.5
		Medial head	TRImed	Humerus	Ulna	624.3
		Lateral head	TRIlat	Humerus	Ulna	624.3
	Anconeus	————————-	ANC	Humerus	Ulna	350.0
Bra	Brachialis	————————-	BRA	Humerus	Ulna	987.3
	Brachioradialis	————————-	BRD	Humerus	Radius	261.3
Bic	Biceps brachii	Long head	BIClong	Scapula	Radius	624.3
		Short head	BICshort	Scapula	Radius	435.6
Sup	Supinator	————————-	SUP	Ulna	Radius	476.0
Pro	Pronator teres	————————-	PT	Humerus	Radius	566.2
	Pronator quadratus	————————-	PQ	Ulna	Radius	75.5

complete motor paraplegia and free of shoulder pain (Table 2) were used. The subjects were recruited from outpatient clinics throughout the Rancho Los Amigos National Rehabilitation Center. The participants provided informed written consent in accordance with the governing institutional review board. Participants propelled their own wheelchair at a self-selected speed on a stationary ergometer with the resistance level set similar to overground propulsion (e.g., Raina et al. 2012). Subjects were allowed to acclimate until they felt comfortable, and then a 10-s trial (preceded by at least 30 s of propulsion to ensure near steady-state propulsion) was recorded. Trunk, right side upper extremity, and wheel kinematics were collected using a 4-scanner CODA motion analysis system (Charnwood Dynamics Ltd., Leicestershire, UK) with 15 markers placed on landmarks on the body and right wheel (e.g., Lighthall-Haubert et al. 2009). Three-dimensional handrim kinetics were measured using an instrumented wheel (SmartWheel; Three Rivers Holdings, Mesa, AZ, USA).

Kinematic and kinetic data were low-pass filtered with a fourth-order zero-lag Butterworth filter with cutoff frequencies of 4 Hz and 8 Hz, respectively, using Visual3D (C-Motion, Inc., Germantown, MD, USA). A resultant handrim force threshold of 5 N was used to delineate between the contact and recovery phases. Contact and recovery phase data for each cycle were time-normalized and averaged across propulsion cycles within each subject. Mean subject data were then averaged across subjects to create group-averaged joint angle and 3D handrim force profiles.

Table 2
Individual and group-averaged subject and propulsion characteristics.

Subject characteristics					Propulsion characteristics		
Subject	Age (years)	Time from injury (years)	Height (m)	Mass (kg)	Full-cycle time (s)	Contact phase time (s)	Propulsion speed (m/s)
1	26.7	4.6	1.68	69.7	0.79	0.28	1.95
2	29.6	9.7	1.75	95.3	1.20	0.48	1.10
3	43.0	16.4	1.75	53.5	0.91	0.35	1.21
4	39.6	15.5	1.70	86.0	0.96	0.36	1.45
5	21.9	6.6	1.83	68.0	1.21	0.33	1.69
6	43.5	16.8	1.73	62.5	1.08	0.36	1.14
7	25.7	2.4	1.73	74.9	1.29	0.37	1.85
8	28.5	6.0	1.73	97.7	1.15	0.38	1.22
9	30.3	15.8	1.68	61.4	1.30	0.48	1.08
10	20.6	2.8	1.85	91.2	1.02	0.35	1.32
11	37.5	15.5	1.70	74.0	1.10	0.44	0.99
12	32.1	16.9	1.73	88.4	1.18	0.41	0.85
Average	**31.6**	**10.7**	**1.74**	**76.9**	**1.10**	**0.38**	**1.32**

2.4. Analysis

Two consecutive propulsion cycles were simulated and the second cycle was analyzed to allow the simulations to reach steady state. Average differences from the group-averaged experimental data were calculated to assess how well each simulation tracked the experimental data. Individual muscle data were analyzed over the full propulsion cycle (contact and recovery). To quantify muscle contributions to propulsion, instantaneous mechanical power (i.e., the product of instantaneous musculotendon force and velocity) was calculated for each muscle at each time step and summed within each muscle group. Mean positive (negative) power generation was calculated by averaging the instantaneous positive (negative) power across time steps, and then total (i.e., absolute value sum) mean power was calculated for each muscle group. Muscle stress was calculated as the instantaneous muscle force at each time step divided by the physiological cross-sectional area and then normalized by the maximum possible isometric stress. This measure of normalized muscle stress is also equivalent to the ratio of the muscle force to the maximum isometric muscle force. Peak and average stress values over the full propulsion cycle were calculated to identify muscle groups that may be at risk for overuse injuries.

Table 3
Root-mean-square differences between the simulated mechanics and group-averaged experimental mechanics. For comparison, one standard deviation (SD) of the experimental data is provided to indicate the inter-subject variability. Baseline denotes the simulation in which no muscle groups were weakened, while the names of the other simulations correspond to the weakened muscle group.

		Joint kinematics (degrees)						Handrim forces (N)			
		Elevation plane	Elevation angle	Shoulder rotation	Elbow flexion	Pronation/supination	All joints	Tangential	Radial	Lateral	All forces
Simulations	Baseline	0.8	0.3	0.8	0.5	0.6	0.6	1.1	1.2	0.4	0.9
	ADelt	0.8	0.3	0.8	0.5	0.6	0.6	1.2	0.9	0.4	0.8
	MDelt	0.8	0.3	0.8	0.5	0.7	0.6	1.1	1.1	0.5	0.9
	Subsc	0.7	0.3	1.2	0.5	0.7	0.7	1.0	1.0	0.5	0.8
	Supra	0.9	0.4	0.8	0.4	0.6	0.6	1.3	1.7	1.6	1.5
	Infra	0.8	0.4	1.6	0.5	0.8	0.8	0.9	1.6	0.9	1.1
	PecMaj	0.8	0.3	0.9	0.5	0.7	0.7	1.3	1.1	0.5	1.0
	Lat	1.0	0.4	2.9	0.5	0.8	1.1	1.2	1.0	0.5	0.9
	Tri	0.8	0.3	0.9	0.5	0.9	0.7	1.1	2.6	0.7	1.4
	Bra	0.8	0.3	0.9	0.4	0.8	0.6	1.2	1.2	0.4	1.0
	Bic	0.8	0.3	0.9	0.5	1.1	0.7	1.1	1.1	0.5	0.9
	Sup	0.8	0.3	0.9	0.5	0.7	0.6	1.1	1.0	0.4	0.8
	Pro	1.0	0.3	0.9	0.4	6.2	1.8	1.1	1.4	0.4	1.0
All simulations		0.8	0.3	1.1	0.5	1.2	0.8	1.1	1.3	0.6	1.0
Experimental variability (1 SD)		17.7	6.7	20.1	10.6	16.7	14.3	6.5	8.9	6.0	7.1

3. Results

All simulations resulted in propulsion mechanics that closely emulated the group-averaged experimental joint kinematics and handrim forces, with average differences of 0.8° and 1.0 N, respectively (Table 3). All root-mean-square (RMS) differences between the simulated and group-averaged experimental mechanics were well within one standard deviation (SD) of the experimental data. The maximum SD-normalized RMS difference (0.37) corresponded to forearm pronation/supination when the pronator group (Table 3: Pro) was weakened. Muscle excitation timings compared well with those reported in the literature (e.g., Mulroy et al. 2004; Rodgers et al. 1994).

3.1. Muscle mechanical power

In general, weakness in individual muscle groups was compensated for by power increases from synergistic groups and decreases from antagonistic groups (Fig. 1, Table 4). The largest power shifts occurred among the shoulder muscles. The largest individual compensation was a power increase from ADelt due to Supra weakness, while the next largest compensation was also a power increase from ADelt but in response to PecMaj weakness. The third largest compensation was a power increase from MDelt due to Subsc weakness.

3.2. Muscle stress

In the baseline simulation, Subsc experienced the highest full-cycle average stress of any muscle group while Supra experienced the second highest level. Supra also experienced the highest full-cycle maximum stress of any muscle group while Infra experienced the second highest level (Fig. 2). On an individual muscle level, subscapularis (SUBSC) experienced the highest average stress and teres minor (TMIN) experienced the highest maximum stress, while supraspinatus (SUPSP) and pronator quadratus (PQ) experienced high levels (both average and maximum).

In general, when individual muscle groups were weakened, the shifts in stress levels (Figs. 3 and 4) corresponded to the shifts in muscle power contributions (Fig. 1). Muscle groups that compensated with increased muscle power generally experienced an increase in stress while muscle groups that compensated by decreasing their power also saw a decrease in stress. Across simulations, the rotator cuff muscle groups (i.e., Subsc, Supra, and Infra) were consistently among the muscle groups with the highest stress levels (Figs. 3 and 4).

4. Discussion

For all the simulations, the optimization framework was able to identify muscle excitation patterns that produced propulsion mechanics

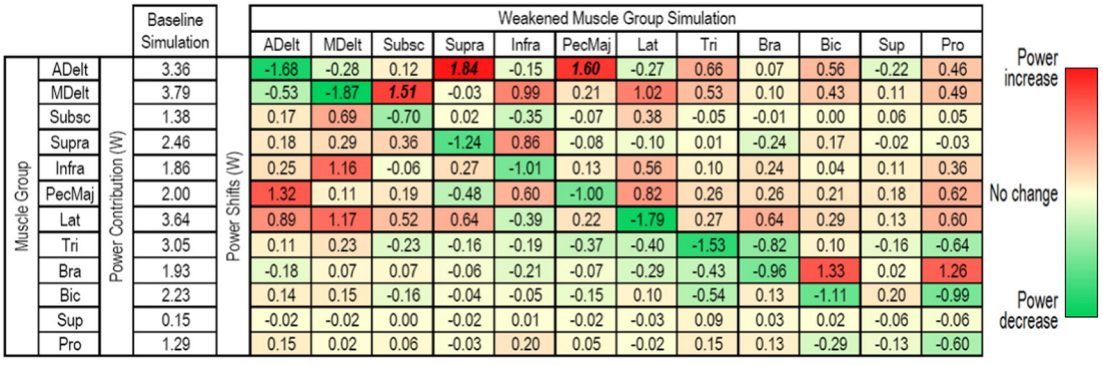

Fig. 1. Total muscle power shifts between muscle groups. Color gradient from red (increase) to green (decrease) represents the change in total muscle power. (For interpretation of the references to color, the reader is referred to the web version of this article). Italics denote a shift greater than 1.50 W.

Table 4
Muscle group power compensations. Key compensations were defined to be those that accounted for at least ten percent of the total magnitude of power shifts that resulted from a muscle group being weakened.

Muscle group weakened	Key compensations	
	Increased power	Decreased power
ADelt	PecMaj, Lat	-----
MDelt	Lat, Infra, Subsc	-----
Subsc	MDelt, Lat	-----
Supra	ADelt, Lat	-----
Infra	MDelt, Supra, PecMaj	-----
PecMaj	ADelt	-----
Lat	MDelt, PecMaj	-----
Tri	ADelt, MDelt	Bic
Bra	Lat	Tri
Bic	Bra, ADelt	-----
Sup	Bic, PecMaj	ADelt, Tri
Pro	Bra, PecMaj	Bic, Tri

that emulated well the group-averaged experimental data. The simulation tracking performance illustrates the ability of the upper extremity muscles to compensate for weakness in individual muscle groups and produce normal (group-averaged) propulsion mechanics.

4.1. Muscle mechanical power

The deltoid and rotator cuff muscle groups (i.e., ADelt, MDelt, Subsc, Supra, and Infra) were among the largest contributors to propulsion. These muscles have also been highlighted as key contributors to generating needed mechanical power in previous simulation (e.g., Rankin et al. 2011) and experimental (e.g., Mulroy et al. 1996) analyses. The large power shifts observed between these muscle groups suggest that they can compensate for each other to restore normal propulsion mechanics, which is consistent with investigations that have found these muscle groups to have similar and overlapping functional capabilities (e.g., Escamilla et al. 2009; Liu et al. 1997).

Although the deltoid and rotator cuff muscles can produce similar moments about the glenohumeral joint, they do so with different combinations of force vectors and moment arms (e.g., Fig. 5). As a result, shifts in contributions between these muscle groups could potentially decrease joint stability and increase injury risk. A previous study investigating the effects of rotator cuff tears highlighted this injury mechanism using an inverse dynamics-based model (van Drongelen et al. 2013). The investigators found that rotator cuff tears, simulated by eliminating the force-generating capacity of the individual muscles, can lead to increased deltoid activity and a more superiorly directed glenohumeral contact force during wheelchair propulsion. This force vector alteration can initiate an injury mechanism in which the humeral head migrates upward into the subacromial space causing rotator cuff impingement. Superior migration of the humeral head after rotator cuff fatigue has also been shown using experimental measurements (e.g., Teyhen et al. 2008).

The thoracohumeral depressors (i.e., PecMaj and Lat) are capable of counteracting this superior humeral head migration and increasing joint stability by drawing the humeral head towards the glenoid fossa (e.g., Oh et al. 2011), with the smaller negative side effect of increased co-contraction due to the associated adduction moment (Steenbrink et al. 2009). Therefore, compensations involving the thoracohumeral depressors are likely preferable compared to those dominated by the deltoid. The distinctions between ADelt and PecMaj in particular may be important as our results also showed that these muscles compensate for each other to provide much of the power required to propel the wheelchair during the contact phase (Fig. 6).

4.2. Muscle stress

While the full-cycle average and maximum stress values may not initially appear high (i.e., the highest muscle group values found in the simulations were 30.4% and 49.1%, respectively), these levels can be significant due to the repetitive nature of wheelchair propulsion. Wheelchair propulsion has a relatively high frequency of about 1 Hz, with approximately 35% of time spent in the contact phase and 65% in the recovery phase (e.g., Mulroy et al. 1996). Although muscles are primarily active during only one phase, rest time is limited due to the task frequency. As a result, levels of muscle intensity and duration similar to those found in this study have previously been identified as risk factors for fatigue and injury (e.g., Monod 1985; Mulroy et al. 1996).

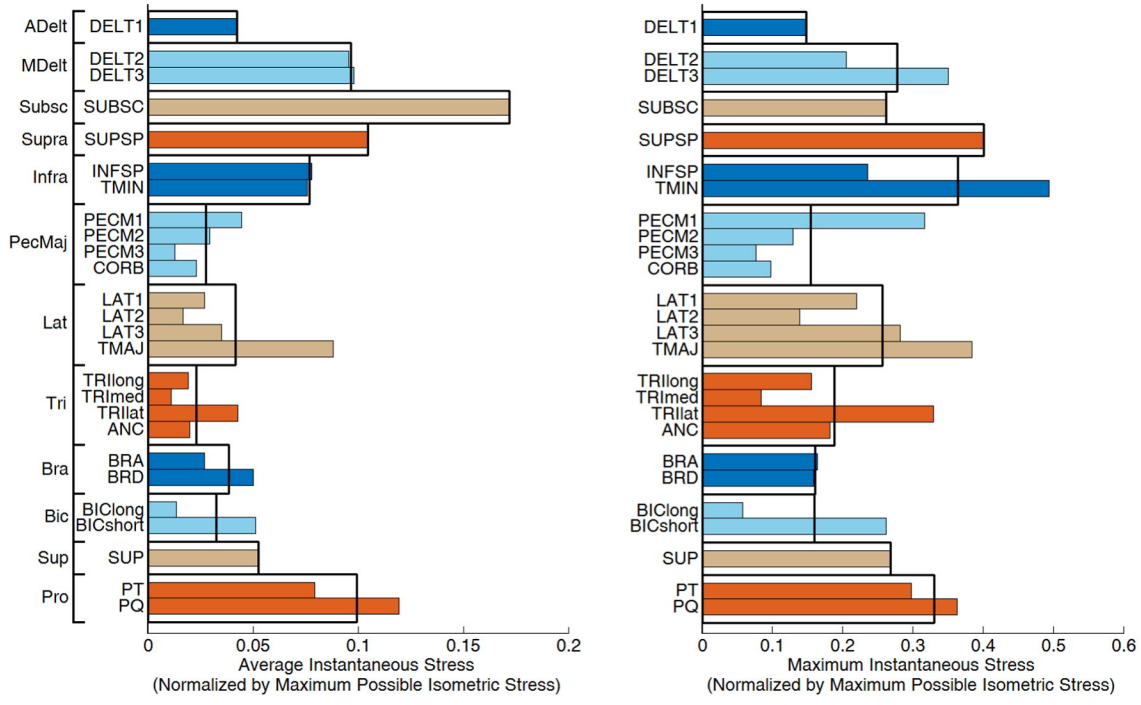

Fig. 2. Baseline simulation average and maximum stress values over the full cycle for the individual muscles. The thick black boxes correspond to the average value for the muscle group.

		Weakened Muscle Group Simulation													
		Baseline	ADelt	MDelt	Subsc	Supra	Infra	PecMaj	Lat	Tri	Bra	Bic	Sup	Pro	Average
ADelt	Full Cycle Average Muscle Stress (%)	4.2	4.2	3.7	3.9	6.6	3.5	6.1	3.9	4.5	4.0	4.3	3.9	4.6	4.4
MDelt		9.7	8.5	9.6	13.9	9.6	11.7	9.9	12.5	10.9	9.8	10.8	9.9	10.7	10.6
Subsc		17.2	19.1	30.4	17.2	16.6	15.3	17.1	19.9	16.6	16.5	16.2	17.8	18.1	18.3
Supra		10.5	11.3	11.7	12.1	10.5	13.7	10.3	10.3	10.6	9.8	11.3	10.4	10.3	11.0
Infra		7.7	7.9	14.7	8.0	8.2	7.7	10.0	17.8	7.7	8.6	6.9	8.0	8.8	9.4
PecMaj		2.7	4.3	4.3	3.2	1.6	3.9	2.8	3.7	3.0	3.2	3.7	2.8	3.9	3.3
Lat		4.2	5.4	5.9	5.1	4.7	3.9	5.1	4.2	4.8	5.1	4.9	4.3	5.1	4.8
Tri		2.3	2.3	2.4	2.1	2.2	2.2	2.1	2.2	2.3	1.7	2.5	2.2	2.3	2.2
Bra		3.9	3.5	4.3	3.6	3.7	3.6	3.4	3.5	2.8	3.9	6.0	3.4	5.8	4.0
Bic		3.2	3.3	3.3	3.1	3.2	3.1	3.1	3.3	2.5	3.6	3.3	3.4	2.1	3.1
Sup		5.2	6.0	5.2	6.5	4.9	6.8	6.0	5.5	9.2	7.1	7.4	5.3	3.6	6.0
Pro		9.9	10.3	11.9	10.4	9.2	9.6	10.5	11.6	10.6	14.6	6.7	6.7	10.5	10.2

Fig. 3. Average stress values over the full cycle for the individual muscle groups. Color gradient from light (low) to dark (high) represents the average stress levels.

The rotator cuff muscles experienced high stress values across the various simulations (including the baseline simulation), which is consistent with previous inverse dynamics-based analyses (Lin et al. 2004; Veeger et al. 2002). These results are also consistent with previous studies suggesting that the rotator cuff muscles are highly active during wheelchair propulsion (e.g., Mulroy et al. 1996; Rankin et al. 2011) and susceptible to fatigue (Newsam et al. 2008). High stress levels could also lead to rotator cuff degeneration and tearing (e.g., Nho et al. 2008), which could further contribute to the power shifts observed above.

Although Pro experienced high stress levels, it also had the lowest muscle power contributions. The high stress levels were primarily due to the relatively small size of these muscles and lack of synergistic muscles to help compensate. The possibility of reducing the amount of pronation while still achieving the propulsive task (e.g., Newsam et al. 1999), along with the low occurrence of pronator injuries and the inherent stability of the pronation/supination degree-of-freedom, suggests that the associated injury risk is much lower for the pronator muscles compared to the rotator cuff muscles.

4.3. Clinical implications

Manual wheelchair users have an elevated risk of rotator cuff injury with tears of the supraspinatus tendon being especially common (Morrow et al. 2014). Glenohumeral joint biomechanics can be affected by rotator cuff injuries and have been found to be critically altered when there is a complete supraspinatus tear (Oh et al. 2011). Rotator cuff injuries are produced by a combination of factors such as muscle stress, overuse and extrinsic mechanisms such as impingement (Seitz et al. 2011). In addition, a recent study has shown that wheelchair users with shoulder muscle weakness, particularly in the shoulder adductors, were more likely to develop shoulder pain over a 3-year period (Mulroy et al. 2015). The design of the upper extremity allows great mobility at the expense of stability and thus requires high muscular effort to prevent superior displacement of the humerus on the glenoid during load-bearing tasks such as wheelchair propulsion (e.g., Mulroy et al. 1996; Veeger and van der Helm 2007). Therefore, strengthening of the rotator cuff muscles and supporting muscles whose contributions do not increase the risk for impingement (i.e., the thoracohumeral depressors), particularly relative to muscles whose contributions do increase this risk (i.e., the deltoid), has the potential to reduce the development of shoulder pain and injury.

4.4. Additional considerations and potential areas for future work

This study explored the effects of weakness in individual muscle groups but did not seek to reproduce a particular source of this weakness. As there are a variety of possible mechanisms leading to muscle weakness, we elected to take a systematic approach, weakening one muscle group at a time to help develop a detailed understanding of potential compensations between muscle groups. A future study could extend this work and seek to replicate common-occurring weakness combinations, such as the denervation of multiple muscle groups due to tetraplegia (e.g., Mulroy et al. 2004) or imbalanced weakness due to the differences in fatiguing rates among shoulder muscles (e.g., Qi et al. 2012).

An additional consideration is that the compensatory strategies identified by the simulations are not the only ones possible. While the identified strategies restore the group-averaged propulsion mechanics while minimizing excess co-contraction, the specific compensatory strategy used by an individual may be influenced by subject-specific differences in muscle capacities and preferred propulsion technique. All subjects in the present study had similar injuries (i.e., all had complete motor paraplegia, as opposed to tetraplegia or one of the numerous

		Weakened Muscle Group Simulation													
		Baseline	ADelt	MDelt	Subsc	Supra	Infra	PecMaj	Lat	Tri	Bra	Bic	Sup	Pro	Average
ADelt	Full Cycle Maximum Muscle Stress (%)	14.8	14.9	14.2	11.9	25.0	11.8	21.3	12.5	13.0	13.6	16.0	12.7	14.3	15.1
MDelt		27.8	26.3	27.3	34.7	28.7	35.1	26.9	33.4	30.5	31.2	28.1	26.5	27.3	29.5
Subsc		26.3	26.5	38.0	26.1	26.5	28.2	24.4	36.1	25.9	26.2	23.1	26.9	26.7	27.8
Supra		40.2	44.7	44.3	44.8	40.0	46.8	43.0	42.1	42.5	40.6	44.9	40.6	39.1	42.6
Infra		36.5	35.3	45.9	20.4	33.3	35.7	39.7	49.1	32.2	33.6	29.2	35.4	34.2	35.4
PecMaj		15.5	19.0	25.9	21.5	7.2	17.2	15.5	23.4	19.1	16.2	20.2	17.2	22.3	18.5
Lat		25.7	26.2	27.2	29.5	25.9	26.9	25.4	25.7	25.9	32.6	25.5	24.4	25.2	26.6
Tri		18.8	19.2	18.2	19.8	16.4	15.5	15.2	17.8	18.9	14.1	17.5	18.9	14.5	17.3
Bra		16.1	13.4	14.8	12.7	12.7	20.7	12.8	20.6	17.5	16.0	19.6	12.6	15.9	15.8
Bic		16.0	16.1	17.5	13.7	15.6	13.9	13.7	15.6	10.5	14.4	16.6	16.9	9.2	14.6
Sup		26.8	39.8	29.4	37.0	28.7	41.1	39.6	29.2	45.6	33.8	37.7	27.9	15.6	33.2
Pro		33.0	35.8	27.4	36.4	35.4	32.5	28.7	33.7	38.1	43.8	23.2	30.5	36.3	33.5

Fig. 4. Maximum stress values over the full cycle for the individual muscle groups. Color gradient from light (low) to dark (high) represents the maximum stress levels.

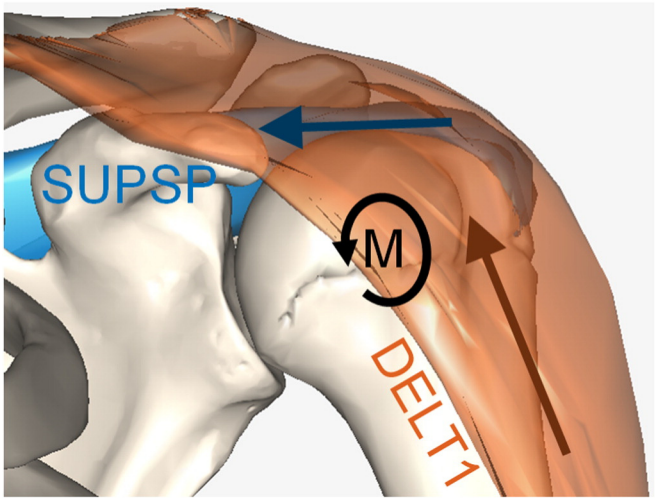

Fig. 5. Moment (M) created by the forces generated by supraspinatus (SUPSP) and anterior deltoid (DELT1). While both muscles can produce an abduction moment, the supraspinatus force draws the humeral head towards the glenoid fossa while the anterior deltoid provides a more superiorly directed force.

other conditions that can lead to wheelchair use) and used a double-loop propulsion pattern (i.e., the propulsion pattern that results when the four commonly observed patterns are averaged; for detailed discussion of these patterns, see Slowik et al. 2015). While the use of a single pattern represented a typical manual wheelchair user while also ensuring low inter-subject variability in propulsion mechanics, care should be taken in extending these results to the entire population of manual wheelchair users.

In addition, it is possible that a subject would modify their propulsion mechanics in response to individual muscle weakness instead of seeking to maintain their original technique. An interesting future study would be to assess the influence of individual muscle weakness on propulsion mechanics and see if it correlates with preferred techniques during a weakened state.

A further consideration is that while the present study identified possible compensatory strategies in the presence of individual muscle weakness and highlighted possible injury mechanisms that may result, it did not attempt to perform a detailed quantitative assessment of joint instability risk, leaving that open as an avenue for future work. The simulations did not allow translation within the glenohumeral joint or include a stability-specific metric in the cost function, but any future study quantitatively examining joint stability should improve stability-related elements of the model and analysis.

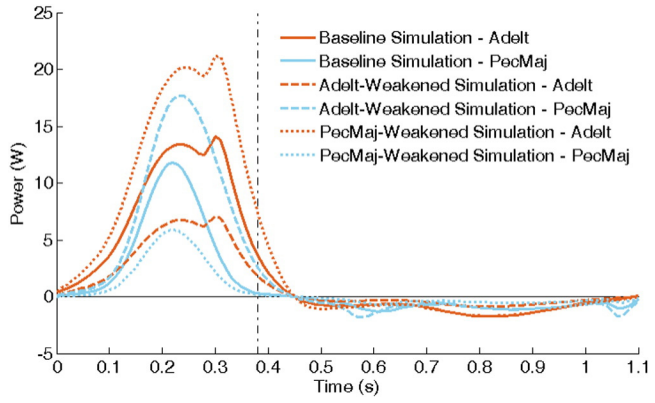

Fig. 6. Instantaneous mechanical power of the Adelt and PecMaj muscle groups for the baseline, Adelt-weakened and PecMaj-weakened simulations. The end of the contact phase is indicated with a vertical line.

4.5. Limitations

A potential limitation in this study is that the experimental data was collected on a calibrated wheelchair ergometer rather than overground. However, while stationary propulsion simulators do not perfectly replicate overground propulsion, they provide greater control over experimental variables in a laboratory setting while still resulting in propulsion mechanics consistent with overground propulsion (Koontz et al. 2012). Thus, the advantage of having steady-state data was deemed to outweigh the limitations the ergometer data may present. Another limitation is that the musculoskeletal model did not include the wrist muscles and the joint was fixed in the anatomical position, thus reducing the ability of the hand to produce a pure moment at the handrim. However, wrist moments are generally small relative to glenohumeral and elbow joint moments (e.g., Robertson et al. 1996; Sabick et al. 2004). In addition, the consistency of the model across all simulations and the requirement that final optimized simulations produce the same experimental joint kinematics and handrim forces minimize the effect of the fixed wrist on the other joints and the study conclusions.

5. Conclusions

In summary, this study identified the effects of individual muscle weakness during manual wheelchair propulsion and highlights the potential risks for the development of upper extremity pain and injury. Despite significant reductions in individual muscle strength, wheelchair propulsion mechanics were able to be restored through compensations from other muscle groups. The largest intermuscular compensations occurred within the shoulder muscles. The simulation results indicate that the deltoid and rotator cuff muscles can produce moments to compensate for each other. However, shifts between these muscles may compromise glenohumeral stability and lead to impingement or other related injuries. Stability can be increased through additional contributions from the thoracohumeral depressors, but with the possible consequence of increased co-contraction. The rotator cuff muscles also experienced many of the highest stress levels across simulations, further highlighting their susceptibility to fatigue and injury. These results highlight the importance of strengthening the rotator cuff muscles and supporting muscles whose contributions do not increase the risk for impingement (i.e., the thoracohumeral depressors) in rehabilitation interventions aimed at minimizing the risk of upper extremity injury in manual wheelchair users.

Conflict of interest statement

The authors have no conflict of interest to declare.

Acknowledgments

This study was supported by NIH grant R01 HD049774 and a National Science Foundation Graduate Research Fellowship under grant DGE-1110007.

References

Burnham, R.S., May, L., Nelson, E., Steadward, R., Reid, D.C., 1993. Shoulder pain in wheelchair athletes. The role of muscle imbalance. Am. J. Sports Med. 21, 238–242.
Curtis, K.A., Drysdale, G.A., Lanza, R.D., Kolber, M., Vitolo, R.S., West, R., 1999. Shoulder pain in wheelchair users with tetraplegia and paraplegia. Arch. Phys. Med. Rehabil. 80, 453–457.
Davy, D.T., Audu, M.L., 1987. A dynamic optimization technique for predicting muscle forces in the swing phase of gait. J. Biomech. 20, 187–201.
de Groot, J.H., Brand, R., 2001. A three-dimensional regression model of the shoulder rhythm. Clin. Biomech. 16, 735–743.
Enoka, R.M., Duchateau, J., 2008. Muscle fatigue: what, why and how it influences muscle function. J. Physiol. 586, 11–23.
Erdemir, A., McLean, S., Herzog, W., van den Bogert, A.J., 2007. Model-based estimation of muscle forces exerted during movements. Clin. Biomech. 22, 131–154.

Escamilla, R.F., Yamashiro, K., Paulos, L., Andrews, J.R., 2009. Shoulder muscle activity and function in common shoulder rehabilitation exercises. Sports Med. 39, 663–685.
Finley, M.A., Rodgers, M.M., 2004. Prevalence and identification of shoulder pathology in athletic and nonathletic wheelchair users with shoulder pain: a pilot study. J. Rehabil. Res. Dev. 41, 395–402.
Goffe, W.L., Ferrier, G.D., Rogers, J., 1994. Global optimization of statistical functions with simulated annealing. J. Econometrics 60, 65–99.
Goldberg, E.J., Neptune, R.R., 2007. Compensatory strategies during normal walking in response to muscle weakness and increased hip joint stiffness. Gait Posture 25, 360–367.
Gutierrez, D.D., Thompson, L., Kemp, B., Mulroy, S.J., 2007. The relationship of shoulder pain intensity to quality of life, physical activity, and community participation in persons with paraplegia. J. Spinal Cord Med. 30, 251–255.
Hall, A.L., Peterson, C.L., Kautz, S.A., Neptune, R.R., 2011. Relationships between muscle contributions to walking subtasks and functional walking status in persons with post-stroke hemiparesis. Clin. Biomech. 26, 509–515.
Happee, R., van der Helm, F.C., 1995. The control of shoulder muscles during goal directed movements, an inverse dynamic analysis. J. Biomech. 28, 1179–1191.
Holzbaur, K.R., Murray, W.M., Delp, S.L., 2005. A model of the upper extremity for simulating musculoskeletal surgery and analyzing neuromuscular control. Ann. Biomed. Eng. 33, 829–840.
Jonkers, I., Stewart, C., Spaepen, A., 2003. The complementary role of the plantarflexors, hamstrings and gluteus maximus in the control of stance limb stability during gait. Gait Posture 17, 264–272.
Koontz, A.M., Worobey, L.A., Rice, I.M., Collinger, J.L., Boninger, M.L., 2012. Comparison between overground and dynamometer manual wheelchair propulsion. J. Appl. Biomech. 28, 412–419.
Kulig, K., Newsam, C.J., Mulroy, S.J., Rao, S., Gronley, J.K., Bontrager, E.L., Perry, J., 2001. The effect of level of spinal cord injury on shoulder joint kinetics during manual wheelchair propulsion. Clin. Biomech. 16, 744–751.
Kumar, S., 2001. Theories of musculoskeletal injury causation. Ergonomics 44, 17–47.
Labriola, J.E., Lee, T.Q., Debski, R.E., McMahon, P.J., 2005. Stability and instability of the glenohumeral joint: the role of shoulder muscles. J. Shoulder Elb. Surg. 14, 32S–38S.
Lighthall-Haubert, L., Requejo, P.S., Mulroy, S.J., Newsam, C.J., Bontrager, E., Gronley, J.K., Perry, J., 2009. Comparison of shoulder muscle electromyographic activity during standard manual wheelchair and push-rim activated power assisted wheelchair propulsion in persons with complete tetraplegia. Arch. Phys. Med. Rehabil. 90, 1904–1915.
Lin, H.T., Su, F.C., Wu, H.W., An, K.N., 2004. Muscle forces analysis in the shoulder mechanism during wheelchair propulsion. Proc. Inst. Mech. Eng. H J. Eng. Med. 218, 213–221.
Liu, J., Hughes, R.E., Smutz, W.P., Niebur, G., Nan-An, K., 1997. Roles of deltoid and rotator cuff muscles in shoulder elevation. Clin. Biomech. 12, 32–38.
Monod, H., 1985. Contractility of muscle during prolonged static and repetitive dynamic activity. Ergonomics 28, 81–89.
Morrow, M.M., Van Straaten, M.G., Murthy, N.S., Braman, J.P., Zanella, E., Zhao, K.D., 2014. Detailed shoulder MRI findings in manual wheelchair users with shoulder pain. Biomed Res Int. 2014, 769649.
Mulroy, S.J., Gronley, J.K., Newsam, C.J., Perry, J., 1996. Electromyographic activity of shoulder muscles during wheelchair propulsion by paraplegic persons. Arch. Phys. Med. Rehabil. 77, 187–193.
Mulroy, S.J., Farrokhi, S., Newsam, C.J., Perry, J., 2004. Effects of spinal cord injury level on the activity of shoulder muscles during wheelchair propulsion: an electromyographic study. Arch. Phys. Med. Rehabil. 85, 925–934.
Mulroy, S.J., Hatchett, P., Eberly, V.J., Haubert, L.L., Conners, S., Requejo, P.S., 2015. Shoulder strength and physical activity predictors of shoulder pain in people with paraplegia from spinal injury: prospective cohort study. Phys. Ther. 95, 1027–1038.
Neptune, R.R., Kautz, S.A., Zajac, F.E., 2001. Contributions of the individual ankle plantar flexors to support, forward progression and swing initiation during walking. J. Biomech. 34, 1387–1398.
Newsam, C.J., Rao, S.S., Mulroy, S.J., Gronley, J.K., Bontrager, E.L., Perry, J., 1999. Three dimensional upper extremity motion during manual wheelchair propulsion in men with different levels of spinal cord injury. Gait Posture 10, 223–232.
Newsam, C.J., Mulroy, S., Perry, J., 2008. Use of power spectral analysis to document shoulder muscle fatigue during 15-minutes of continuous manual wheelchair propulsion. J. Spinal Cord Med. 31, 231.
Nho, S.J., Yadav, H., Shindle, M.K., Macgillivray, J.D., 2008. Rotator cuff degeneration: etiology and pathogenesis. Am. J. Sports Med. 36, 987–993.
Oh, J.H., Jun, B.J., McGarry, M.H., Lee, T.Q., 2011. Does a critical rotator cuff tear stage exist?: a biomechanical study of rotator cuff tear progression in human cadaver shoulders. J. Bone Joint Surg. Am. 93, 2100–2109.
Pandy, M.G., Andriacchi, T.P., 2010. Muscle and joint function in human locomotion. Annu. Rev. Biomed. Eng. 12, 401–433.
Qi, L., Wakeling, J., Grange, S., Ferguson-Pell, M., 2012. Changes in surface electromyography signals and kinetics associated with progression of fatigue at two speeds during wheelchair propulsion. J. Rehabil. Res. Dev. 49, 23–34.
Raasch, C.C., Zajac, F.E., Ma, B., Levine, W.S., 1997. Muscle coordination of maximum-speed pedaling. J. Biomech. 30, 595–602.
Raina, S., McNitt-Gray, J., Mulroy, S., Requejo, P., 2012. Effect of choice of recovery patterns on handrim kinetics in manual wheelchair users with paraplegia and tetraplegia. J. Spinal Cord Med. 35, 148–155.
Rankin, J.W., Neptune, R.R., 2012. Musculotendon lengths and moment arms for a three-dimensional upper-extremity model. J. Biomech. 45, 1739–1744.
Rankin, J.W., Kwarciak, A.M., Mark Richter, W., Neptune, R.R., 2010. The influence of altering push force effectiveness on upper extremity demand during wheelchair propulsion. J. Biomech. 43, 2771–2779.
Rankin, J.W., Richter, W.M., Neptune, R.R., 2011. Individual muscle contributions to push and recovery subtasks during wheelchair propulsion. J. Biomech. 44, 1246–1252.
Rankin, J.W., Kwarciak, A.M., Richter, W.M., Neptune, R.R., 2012. The influence of wheelchair propulsion technique on upper extremity muscle demand: a simulation study. Clin. Biomech. 27, 879–886.
Requejo, P., Mulroy, S., Haubert, L.L., Newsam, C., Gronley, J., Perry, J., 2008. Evidence-based strategies to preserve shoulder function in manual wheelchair users with spinal cord injury. Top. Spinal Cord Inj. Rehabil. 13, 86–119.
Rice, I., Impink, B., Niyonkuru, C., Boninger, M., 2009. Manual wheelchair stroke characteristics during an extended period of propulsion. Spinal Cord 47, 413–417.
Robertson, R.N., Boninger, M.L., Cooper, R.A., Shimada, S.D., 1996. Pushrim forces and joint kinetics during wheelchair propulsion. Arch. Phys. Med. Rehabil. 77, 856–864.
Rodgers, M.M., Gayle, G.W., Figoni, S.F., Kobayashi, M., Lieh, J., Glaser, R.M., 1994. Biomechanics of wheelchair propulsion during fatigue. Arch. Phys. Med. Rehabil. 75, 85–93.
Rodgers, M.M., McQuade, K.J., Rasch, E.K., Keyser, R.E., Finley, M.A., 2003. Upper-limb fatigue-related joint power shifts in experienced wheelchair users and nonwheelchair users. J. Rehabil. Res. Dev. 40, 27–37.
Sabick, M.B., Kotajarvi, B.R., An, K.N., 2004. A new method to quantify demand on the upper extremity during manual wheelchair propulsion. Arch. Phys. Med. Rehabil. 85, 1151–1159.
Seitz, A.L., McClure, P.W., Finucane, S., Boardman 3rd, N.D., Michener, L.A., 2011. Mechanisms of rotator cuff tendinopathy: intrinsic, extrinsic, or both? Clin. Biomech. 26, 1–12.
Sharkey, N.A., Marder, R.A., 1995. The rotator cuff opposes superior translation of the humeral head. Am. J. Sports Med. 23, 270–275.
Slowik, J.S., Neptune, R.R., 2013. A theoretical analysis of the influence of wheelchair seat position on upper extremity demand. Clin. Biomech. 28, 378–385.
Slowik, J.S., Requejo, P.S., Mulroy, S.J., Neptune, R.R., 2015. The influence of speed and grade on wheelchair propulsion hand pattern. Clin. Biomech. 30, 927–932.
Steenbrink, F., de Groot, J.H., Veeger, H.E., van der Helm, F.C., Rozing, P.M., 2009. Glenohumeral stability in simulated rotator cuff tears. J. Biomech. 42, 1740–1745.
Teyhen, D.S., Miller, J.M., Middag, T.R., Kane, E.J., 2008. Rotator cuff fatigue and glenohumeral kinematics in participants without shoulder dysfunction. J. Athl. Train. 43, 352–358.
Thomas, C.K., Zijdewind, I., 2006. Fatigue of muscles weakened by death of motoneurons. Muscle Nerve 33, 21–41.
van der Helm, F.C., Veeger, H.E., 1996. Quasi-static analysis of muscle forces in the shoulder mechanism during wheelchair propulsion. J. Biomech. 29, 39–52.
van der Krogt, M.M., Delp, S.L., Schwartz, M.H., 2012. How robust is human gait to muscle weakness? Gait Posture 36, 113–119.
van Drongelen, S., van der Woude, L.H., Janssen, T.W., Angenot, E.L., Chadwick, E.K., Veeger, H.E., 2006. Glenohumeral joint loading in tetraplegia during weight relief lifting: a simulation study. Clin. Biomech. 21, 128–137.
van Drongelen, S., Schlussel, M., Arnet, U., Veeger, D., 2013. The influence of simulated rotator cuff tears on the risk for impingement in handbike and handrim wheelchair propulsion. Clin. Biomech. 28, 495–501.
Veeger, H.E., van der Helm, F.C., 2007. Shoulder function: the perfect compromise between mobility and stability. J. Biomech. 40, 2119–2129.
Veeger, H.E., van der Woude, L.H., Rozendal, R.H., 1991. Load on the upper extremity in manual wheelchair propulsion. J. Electromyogr. Kinesiol. 1, 270–280.
Veeger, H.E., Rozendaal, L.A., van der Helm, F.C., 2002. Load on the shoulder in low intensity wheelchair propulsion. Clin. Biomech. 17, 211–218.
Winters, J.M., Stark, L., 1988. Estimated mechanical properties of synergistic muscles involved in movements of a variety of human joints. J. Biomech. 21, 1027–1041.
Zajac, F.E., Neptune, R.R., Kautz, S.A., 2002. Biomechanics and muscle coordination of human walking. part I: introduction to concepts, power transfer, dynamics and simulations. Gait Posture 16, 215–232.